TB67

19th International Symposium of Ballistics, 7–11 May 2001, Interlaken, Switzerland

THE EFFECT OF OBLIQUITY AND CONDUCTIVITY ON THE CURRENT DISTRIBUTIONS WITHIN AN ELECTRIC ARMOUR

D. J. R. Swatton[1], D. C. Pack[2], J. Brown[1], P. C. Endersby[1] and P. R. Ratcliff[1]

[1] DERA, Fort Halstead, Sevenoaks, Kent, TN14 7BP, UK
[2] Department of Mathematics, University of Strathclyde, Glasgow, Scotland

At Ballistics 99, the authors' paper examined analytically the flow of current into and out of jets orthogonal to electric armour. Near-rotational symmetry was observed, irrespective of supply geometry. It was thus suggested that the pairs of large, opposed off-axis forces sometimes observed in experiments must only appear when the jet is oblique to the target. This rotational symmetry is here shown to persist for electrodes of any conductivity. *Oblique* passage of jets through electrified plates is examined in a further development of our model. We represent electrodes by infinite half-spaces, but calculation shows that current is in fact naturally confined within the envelopes of practicably sized plates. The geometries chosen thus offer reasonable representations of jet, supply, and electrode currents at practicable frequencies, whilst still offering soluble formulations of the relevant Maxwell's equations. The computed electrode currents are presented in graphical form.

INTRODUCTION

Electric Armour in its simplest form can consist of two parallel conductive plates connected to opposite poles of a charged high-energy capacitor. An incoming shaped charge jet can act as the switch. When touchdown on the second electrode occurs, large currents are able to flow, which cause disruption of the jet.

The principal mechanism is magnetohydrodynamic (MHD) pinch, which causes successive segments of the jet to expand rapidly into diffuse toroidal structures [1,2] (Fig. 1). A secondary mechanism is lateral dispersion of the jet by off-axis forces arising from interaction of the jet current with the electrodes' magnetic fields (Fig. 1). This effect is often slight. But in some cases, pairs of relatively large opposed forces have been observed; photographs in [3] showed severely bent surrogate jet segments in tests.

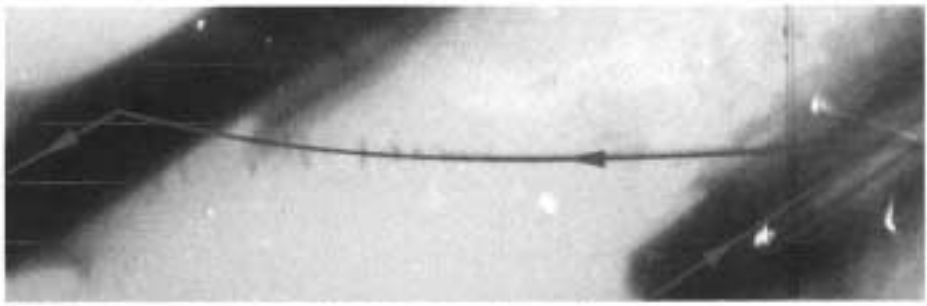

Figure 1. Radiograph of a shaped charge jet penetrating an electric armour array. Motion is from right to left and arrows represent the *notional* flow of current.

In [3], the possible role of current supply geometry was examined by modelling the distribution of currents in perfectly conducting electrodes. It was concluded that current flow in and out of orthogonal jets was substantially rotationally symmetrical, irrespective of current supply. The only off-axis forces detected were due to a weak 'railgun effect', acting in the same direction and with the same magnitude all along the jet. It was then suggested that jet orientation, rather than the details of current supply, must be the source of the large bending moments observed in the experiments. Here, the possible influence of finite conductivity in the electrodes is first checked, again in orthogonal geometry. Body currents replace the surface currents evaluated in [3]. In oblique geometry, large asymmetries *are* found. The proximity effect turns out to affect the distribution of current in the electrodes, and hence the forces acting on jets.

The origin of off-axis forces

The current distributions within the electrodes may be visualised in terms of elements, defined by $\mathbf{J}dV$, representing the proportion of the total current flowing through an infinitesimal volume, dV. The Biot-Savart law [4] gives the magnetic field due to the current in the whole of the electrode at any point with position vector $\mathbf{r}$ relative to $\mathbf{J}dV$ as:

$$\mathbf{B} = \int_V \frac{\mu_0 \mathbf{J} \times \mathbf{r}}{4\pi r^3} dV \,. \tag{1}$$

The cross product in (1) implies that the magnetic field associated with each current filament is rotationally symmetrical about $\mathbf{J}$. By considering the complete current distribution as the sum over an infinite number of current elements, it follows that the magnetic field external to an electrode will be wrapped around the plate. The force on any current filament deseribed by $r = r(s)$ in the magnetic field of the plate is given by $\mathbf{dF} = I\delta(r - r(s))\mathbf{dl} \times \mathbf{B}$ [4]. In general, the jet and $\mathbf{B}$ are not parallel, implying that the resultant force per unit length on any segment of current carrying jet *must be at right angles to its axis.*

FINITE CONDUCTIVITY

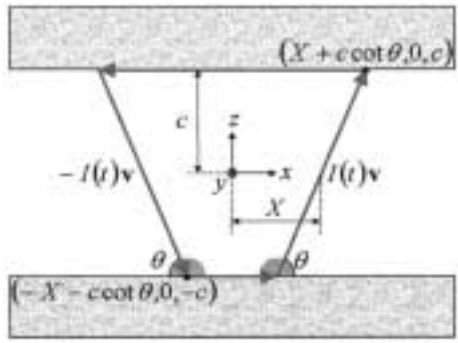

Figure 2. Modelling current distribution (generalised jet/electrode geometry).

The model geometry in this case follows Fig. (2). Two infinite conductors separated by a vacuum are connected by two perpendicular (i.e. $\theta = \rho/2$) filaments carrying currents, $\pm I(t)$.

Modelling the electrodes as half-spaces, with just three regions in *xyz*-space to consider, simplifies the solution of Maxwell's equations. Edge effects can be neglected if the jet is many times its own diameter distant from the electrode boundaries.

The fact that there are two filaments is important. One represents the jet as it passes through the electric armour. The second is partly an artificial construct, providing a return path to prevent build-up of charge. However, the 'dummy' jet is also the image current of the real jet, so current density vectors become parallel to each other, and perpendicular to the intersection of the symmetry plane and the electrodes. It is felt that this provides an acceptable representation of the supply to real electrodes.

With finite conductivity, in general there will be a non-zero electric field within the plates. Thus Maxwell's equations must be solved in all three regions. Instead of surface currents, body currents, $\mathbf{J}_{\pm}$, flow (the + and – denoting the two electrodes).

Governing equations

Maxwell's equations, which govern the *xyzt*-dependence of the electromagnetic fields, written in terms of a scalar and vector potential, φ and $\mathbf{A}$ respectively are [3, 5]:

$$\nabla^2\varphi_i = -\rho_i/e_{r,i}\,,\quad \nabla^2\mathbf{A}_i = -\mu_{r,i}\mathbf{J}_i \quad \text{and} \quad \nabla\cdot\mathrm{A}_i = (\delta_{i,2}-1)\mu_{r,i}\sigma\varphi_i. \tag{2}$$

The subscript i, running from 1 to 3, denotes the three regions, upper electrode, vacuum and lower electrode. $\delta_{i,j}$ represents Kronecker's symbol defined as 0 unless $i = j$ when it is unity. The first two are Poisson-type equations, their right hand sides acting as source terms generating the electromagnetic fields. There is no free charge in the system, so $\rho = 0$. Using the Dirac delta function, δ, the current filaments are defined as

$$\mathbf{J} = I(t)\delta(y)\{\delta(\mathrm{x}-\mathrm{X})\mathbf{k} - \delta(x-\mathrm{X})\mathbf{k}\}. \tag{3}$$

The third equation in (2) is the gauge condition. Like constants of integration in the solution of differential equations, there is freedom to select this. The choice of gauge for the electrodes is different to that for the vacuum; it is informed by a wish to decouple the 2nd-order equations.

Boundary conditions complete the specification of the model, they are:

$$\varphi, \mathbf{A}, \partial_x\varphi, \partial_y\varphi, \partial_x\mathbf{A}, \partial_y\mathbf{A} \to 0 \quad \text{as} \quad x, y \to \pm\infty, \tag{4}$$

$$[\varphi]_{z=\pm c} = 0, \quad \mathbf{k} \times [\mathbf{A}]_{z=\pm c} = 0, \tag{5}$$

$$\mathbf{k} \cdot [\varepsilon_r \nabla\varphi]_{z=\pm c} + \mathbf{k} \cdot [\varepsilon_r \partial_t \mathbf{A}]_{z=\pm c} = \mp\rho_{s\pm} \quad \text{and} \quad \mathbf{k} \times \left[\frac{1}{\mu_r}\mathbf{A}\right]_{z=\pm c} = 0. \tag{6}$$

Here [ ] denotes the change in a dependent variable across the bonndaries; the quantity $\rho_{s\pm}$ represents the surface charge admissible by Maxwell's equations. Equation (4) states that far away from the region of interest, an observer is unaware of any disturbances in the electromagnetic continuum. Equations (5) and (6) are representations of the standard 'jump conditions' that define the changes in **E** and **B** across a boundary between two different materials [2, 6].

Solution

The method of solution is very similar to that of Tegepoulos and Kriezis [7]: $\mathbf{A}_2$, the vector potential in the vacuum, is split into two components, the first of which represents that generated by the two filaments. The second represents the response due to the eddy currents generated within the two electrodes. Fourier transform techniques are used to solve equations (2).

Results: finite conductivity

Obviously, due to the 3-D nature of the current distributions, a direct comparison with the results presented in [3] is not possible. In a steady state, the current flowing on the surface of e plates is shown in Figure (3). The near-rotational symmetry of current flows around the ends of the filaments is retained. In this case, as before, off-axis forces due to the asymmetry in the current supply are small, and constant along the filaments.

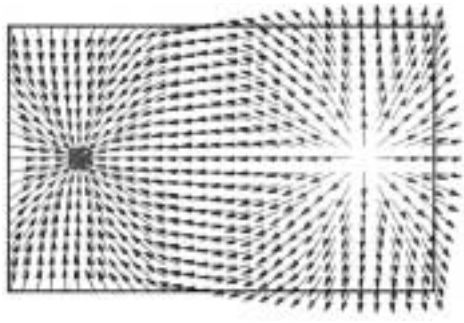

Figure 3. Current distribution on the surfaces of electrodes of finite conductivity connected by orthogonal filaments.

OBLIQUE GEOMETRY

In the more general, oblique, geometry there may be other contributing parameters as well as those due to asymmetric current supplies. For one thing, each jet segment must travel more nearly parallel to one electrode (at the acute junction), and therefore experience greater magnetic fields than in the orthogonal case. Furthermore, current may be

attracted, due to the so-called 'proximity effect', into that zone of the electrode where jet meets it at an acute angle. This would further increase the magnetic field experienced by the jet. It was conjectured that these effects might act in synergy. Confirmation of this is now presented.

The model geometry for considering oblique filaments is as in Fig. (2). Perfectly conducting electrodes effectively reduce to one the number of regions in which Maxwell's equations need to be solved. Electrode currents will flow on the surfaces.

Governing equations

In this case, Maxwell's equations within the vacuum are:

$$\nabla^2\varphi_2 = -\rho/\varepsilon_0\,, \quad \nabla^2\mathbf{A}_2 = -\mu_0\mathbf{J} \quad \text{and} \quad \nabla\cdot\mathbf{A}_2 = 0\,, \tag{7}$$

where again it will be assumed that $\rho = 0$, but now

$$\begin{aligned}\mathbf{J} = I(t)\delta(y)\{&\delta(x-(X+z\cot\theta))\{\cos\theta\mathbf{i}+\sin\theta\mathbf{k}\}\\ &+\delta(x-(X+z\cot\theta))\{\cos\theta\mathbf{i}+\sin\theta\mathbf{k}\}\}\end{aligned} \tag{8}$$

defining mathematically the two angled current filaments illustrated in Fig. 2.

Simpler equations govern the scalar and vector potentials in the electrodes. Since within a perfect conductor $\mathbf{E} = \mathbf{B} = \mathbf{J} = 0$ [8], with a particular choice of gauge it can further be shown that:

$$\mathbf{A}_{1,3} = 0, \quad \varphi_1 = f_+(t) \quad \text{and} \quad \varphi_3 = f_-(t)\,. \tag{9}$$

Boundary conditions are needed to complete the formulation. At infinity, equation (4) is again used. Using equation (9), the 'jump conditions' of (5) and (6) simplify to:

$$\varphi_2\big|_{z=\pm c} = f_\pm(t), \quad \mathbf{k}\times\mathbf{A}_2\big|_{z=\pm c} = 0\,, \tag{10}$$

$$\mathbf{k}\cdot\nabla\varphi_2\big|_{z=\pm c} + \mathbf{k}\cdot\partial_t\mathbf{A}_2\big|_{z=\pm c} = \pm\rho_{s\pm}/\varepsilon_0 \quad \text{and} \quad \mathbf{k}\times\mathbf{A}_2\big|_{z=\pm c} = \mp\mu_0\mathbf{J}_{S\pm}\,. \tag{11}$$

Note the existence of a surface current, $\mathbf{J}_{S\pm}$ representing the electrode current.

Method of solution

A solution to equations (7), (8), (10) and (11) is again found using Fourier Transform techniques. Multiplying equations (5) by $e^{-i\alpha x}e^{-i\beta y}$ and integrating yields second order linear differential equations in z, parameterisod by α and β.

The solution obtained is made to fit the boundary conditions. In practice, only the gauge condition and equations (10) are needed to determine the unknowns. (11) simply provides a way of obtaining expressions for the surface charge and current distributions.

Results: oblique geometry

The calculated current distributions on the upper and lower electrodes are plotted in Figures (4) and (5).

In the example shown, electrodes are spaced apart by a distance equal to half of the separation of the midpoints of the two filaments. The components of each vector are inverse Fourier transforms. These have been calculated numerically using the commercial package Mathematica 4. The required integration ranges, $0 < \alpha < \infty$ and $0 < \beta < \infty$ have been approximated by $0 < \alpha < 100$ and $0 < \beta < 100$ to reduce run-time.

The somewhat unphysical abrupt excursions in numerical values visible in places arise from modelling the filament currents as lines. Strictly, from (8), current density between the plates should exhibit singular behaviour proportional to the sum of $\delta(y)\delta(x - (X + z_{cot}\theta))$ and $\delta(y)\delta(x - (X + z_{cot}\theta))$. This promotes similar behaviour in $\mathbf{A}_2$. In order for Fourier transforms to be able to respond correctly to this impulse-like behaviour, the complete domain, i.e. $(0,\infty) \times (0,\infty)$, ought to be used as opposed to the restricted domain. This, however, is incompatible with numerical methods of inverting the transformation Note that although Fourier transforms were used to compute the current distributions in the finite-conductivity case earlier in the paper, unphysical behaviour did not then occur, since closed forms of the inverse transformations existed.

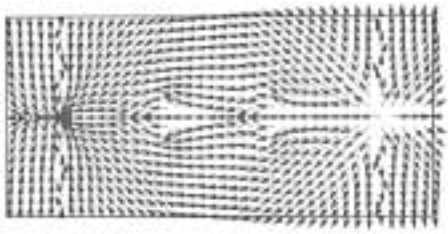

Figure 4. Current distribution on the upper electrode.

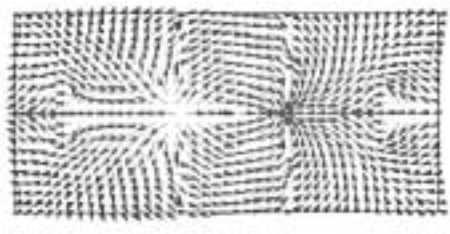

Figure 5. Current distribution on the lower electrode.

CONCLUSIONS

1. Conductivity

The solution for electrodes of finite conductivity differs somewhat from the work reported previously, due to the finite electric field between the plates. However despite the existence of *z*-components in the plate currents, examination of the current density on the electrode surfaces suggests that the near-radial symmetry about the jets presented in [3] is retained. Also as in [3], the magnetic field is found to be equivalent to that generated by two infinitely long filaments, supporting the suggestion that any substantial off-axis forces, when observed in practice, must largely arise due to asymmetries in the jet/plate interaction geometry.

2. Oblique jet

The marked asymmetry in the current plots in oblique geometry accords qualitatively with the experimentally observed direction and magnitude of jet bending.

At each acute junction between jet and electrode, the close proximity of the angled jet causes extra current to be drawn into nearby regions of the electrode. Asymmetries in the current distributions, and hence of the magnetic fields, near the junctions are thus even greater than intuition might suggest. Highly unbalanced forces act upon the jet during its passage, tending always to drive it away from the regions of high current density in the electrodes. This explains the S-shaped form into which surrogate copper jets were bent in the static expenments reported in [3].

ACKNOWLEDGEMENT

The other authors wish to record their good wishes to Professor D. C. Pack on the occasion of his eightieth birthday, and his nearly 60 years in hydrodynamics research.

This ranges from his formulation of the Root Density Law in World War II to the present work.

REFERENCES

1. J. Brown and P. C. Endersby, "Electric Armour Research in the UK", *2nd International All-Electric Vehicle Conference, Detroit, Mi,* 333–343, l997.
2. D. L. Littlefield and J. D. Powell, "The Effect of Electromagnetic Fields on the Stability of a Uniformly Plastic Jet", *Phys. Fluids A2(12)* 2240–2248, 1990.
3. D. J. R. Swatton, J. Brown, P. C. Endersby, P. R. Ratcliff, D. C. Pack and R. J. Cliffe, "Influence of different topologies in electric armour", *presented at the 18th International Symposium on Ballistics, San Antonio, Texas,* 1999.
4. W. J. Duffin, "EIectricity and magnetism", *McGraw-Hill Book Co. (UK) Ltd., Maidenhead, 3rd edition,* 1980.
5. C. J. Carpenter, "Comparison of alternative formulations of 3-dimensional magnetic-field and eddy-current problems at power frequencies", *Proc. IEE Vol. 124,* No. 11, 1026, 1977.
6. M. Kruskal and M Schwarzschild, "Some instabilities of a completely ionized plasma", *Proc. R Soc. London Ser. A 223,* 348–360, 1954.
7. J. A. Tegopoulos and M. Kriezis, "Eddy currents in linear conducting media", *Elsevier, Amsterdam,* 1985.
8. P. Moon and D. E. Spencer, "Foundations of electrodynamics", *D. Van Nostrand Company, Inc.*, 1960.